NJC

Accepted Manuscript

This is an *Accepted Manuscript*, which has been through the Royal Society of Chemistry peer review process and has been accepted for publication.

Accepted Manuscripts are published online shortly after acceptance, before technical editing, formatting and proof reading. Using this free service, authors can make their results available to the community, in citable form, before we publish the edited article. We will replace this *Accepted Manuscript* with the edited and formatted *Advance Article* as soon as it is available.

You can find more information about *Accepted Manuscripts* in the Information for Authors.

Please note that technical editing may introduce minor changes to the text and/or graphics, which may alter content. The journal's standard Terms & Conditions and the Ethical guidelines still apply. In no event shall the Royal Society of Chemistry be held responsible for any errors or omissions in this *Accepted Manuscript* or any consequences arising from the use of any information it contains.

ROYAL SOCIETY OF CHEMISTRY

www.rsc.org/njc

Journal Name

ARTICLE

Design, synthesis, linear and nonlinear photophysical properties of novel pyrimidine-based imidazole derivatives

Received 00th January 20xx,
Accepted 00th January 20xx

DOI: 10.1039/x0xx00000x

www.rsc.org/

Qiong Zhang[a,b], Lei Luo[c], Hong Xu[a], Zhangjun Hu[d], Caroline Brommesson[d], Jieying Wu[a], Zhaoqi Sun[b*], Yupeng Tian[a*] and Kajsa Uvdal[d]

A novel donor-π-acceptor (D-π-A) and donor-π-acceptor-π-donor (D-π-A-π-D) type pyrimidine imidazole derivatives with flexible ether oxygen chain molecules (L1 and L2) have been efficiently synthesized through improved Knoevenagel condensation and Ullmann reactions with high yield. Based on systematic photophysical investigations and theoretical calculations, the structure-property relationships can be drawn as follows: (1) The linear and nonlinear optical properties of the target chromophores change regularly with increasing the number of branches and the polarity of solvents. (2) One-substituted chromophore L2 exhibited remarkable negative solvato-kinetic effect, while two-substituted chromophore L1 showed positive solvato-kinetic effect. Significant bathochromic shifting of the emission spectra and larger Stokes shifts were observed in polar solvents. (3) The two-photon absorption (TPA) cross-section results further demonstrated that their TPA cross section values (*δ*) increase notably with increasing branch number, as well as the presence of high π-delocalization could induce large size-scalable TPA enhancements. (4) Comprehensively considered the optical performance, cytotoxicity and solubility, L1 was identified to be the better candidate for living cells (HepG2) imaging.

Introduction

Two-photon excitation (TPE) has become particular practical significance because of the development of highly efficient two-photon absorbing (TPA) materials and their applications. Organic materials with striking TPA effect and large TPA cross- section have attracted considerable attention. Novel large two-photon-active materials, which play an important role in the current field of the non-linear optical materials, have attracted more and more attentions from chemists, material scientists and biophysicists, owing to their applications in many fields, such as optical limiting [1,2], two-photon photodynamic therapy [3,4], two-photon excited fluorescence microscopy [5,6], three-dimensional(3D) optical data storage [7-9], 3D microfabrication [10,11] and so on. To realize these applications, recent research encompassing synthesis, structures and theory have revealed the importance of certain basic structural motifs for TPA-active organic materials [12–17]. Many pioneers believe and demonstrate the conjugation length, donor and acceptor, and planarity of the center are important parameters for symmetric charge displacement upon excitation, which enhance ultimately the TPA cross-section [18–22]. By combining experiments with theory, Prasad *et al*. [20] and Goodson *et al*. [24] found that triphenylamine-cored branched molecules with alkene π-bridges show exceptionally large TPA cross-sections. Cho *et al*. [25] have shown theoretically that, in branched molecules, the TPA cross-section increases as the strength of the donor–acceptor interaction increases.

Pyrimidine, as a heterocycle molecule, has high electron affinity and good coplanarity making it an appropriate building block in construction of chromophores for nonlinear optical materials. [26-27]. Recently, several TPA chromophores utilizing pyrimidine as an electron-withdrawing central core substituent have been synthesized, and fairly good values of TPA cross section have been

[a] Department of Chemistry, Anhui University, Hefei 230039 (P. R. China) Fax: (+86) 551-63861152 E-mail: yptian@ahu.edu.cn

[b] School of Physics and Material Science, Anhui University, Hefei 230601, P. R. China E-mail:szq@ahu.edu.cn

[c] College of Pharmaceutical Science, Southwest University, China, 400715

[d] Division of Molecular Surface Physics & Nanoscience, Department of Physics, Chemistry and Biology (IFM), Linköping University, 58183 Linköping (Sweden)
Electronic Supplementary Information (ESI) available: See DOI: 10.1039/x0xx00000x

measured for them[28]. Meanwhile, pyrimidine are found in many natural products which are the important constituents of a number of modern drugs. It exhibited an adequate safety, tolerability and clinical efficacy profile in preclinical and clinical trials[29]. The methyl groups located in position 4 and 6 of the pyrimidine core have a well-known reactivity,which can easily undergo reactions with an aromatic aldehyde under solvent-free conditions.On the other hand, Flexible ether oxygen chain can not only increase the solubility of the molecule, but also enhance the extent of electron delocalization and ability of the TPA compound to donate electrons.

Furthermore, combined with previous work[30], two novel pyrimidine derivatives with flexible ether oxygen chain are investigated in this work. When these molecules have similar framework, such as bent-shaped D-π-A-π-D chromophore molecules, one can observe that the nature of peripheral substituting groups (D) have significant influence on their fluorescence properties. In this work, it can be safely concluded that a novel Λ-type pyrimidine-based imidazole quadrupolar derivative consisting of a strong pyrimidine electron-accepting center and an electron-donating end group linked through a π-conjugated bridge have proved to be excellent TPA materials, which demonstrate that good coplanarity of the conjugated system, high π-delocalization, and additional cooperative enhancement of the two branches play an important role in the non-linear optical materials. Finally, we found successfully that L1 to be an efficient TP imaging reporter for detection of organelle- and tumor cell with high spatial resolution in HepG2 cells.

Experimental section

1 General procedure

Chemicals were purchased and used as received. Every solvent was purified by conventional methods beforehand. The solvents were dried and distilled according to standard procedures. The synthetic routes for the compounds are presented in Figure 1. All of the reactions were monitored by TLC (silica gel plates, GF254). Silica gel 60 (200–300 mesh) was used for column chromatography. IR spectra were recorded with a Nicolet FT-IR NEXUS 870 spectrometer (KBr discs) in the 4000–400 cm^{-1} region. ^{1}H and ^{13}C NMR spectra were recorded on a 400 or 500 MHz NMR instrument using $CDCl_3$ or $(CD_3)_2SO$ as the solvent. Chemical shifts were reported in parts per million (ppm) relative to TMS (0 ppm) and coupling constants in Hz. Splitting patterns were described as singlet (s), doublet (d), triplet (t), quartet (q), or multiplet (m). The mass spectra were obtained on a Bruker Autoflex III smartbeam mass spectrometer and a Finnigan LCQ Spectrometer.

2 Optical measurements

The one-photon absorption (OPA) spectra were recorded on a SPECORD S600 spectrophotometer. The one-photon excited fluorescence (OPEF) spectra measurements were performed using a Hitachi F-7000 fluorescence spectrophotometer. The OPA and OPEF spectra of compounds L1 and L2 were measured in seven organic solvents of different polarities with a concentration of 1.0×10^{-6} mol L^{-1}. The quartz cuvettes used had a 1 cm path length. The fluorescence quantum yields (φ) were determined by using fluorescein as the reference according to the literature method [31].Quantum yields were corrected as follows:

$$\Phi_s = \Phi_r \left(\frac{A_r \eta_s^2 D_s}{A_s \eta_r^2 D_r}\right)$$

Where the *s* and *r* indices designate the sample and reference samples, respectively; A is the absorbance at λ_{exc}; *h* is the average refractive index of the appropriate solution; and *D* is the integrated area under the corrected emission spectrum.

For time-resolved fluorescence measurements, the fluorescence signals were collimated and focused onto the entrance slit of a monochromator with the output plane equipped with a photomultiplier tube (HORIBA HuoroMax-4P). The decays were analyzed by the 'least-squares' method. The quality of the exponential fits was evaluated by the goodness of fit (χ^2).

TPA cross-section (δ): TPEF spectra were measured using femtosecond laser pulse and Ti: sapphire system (680-1080 nm, 80 MHz, 140 fs) as the light source. All measurements were carried out in air at room temperature. The sample was at a concentration of 1.0×10^{-3} mol L^{-1}. The intensities of the TPEF spectra of the reference and the sample were determined at their excitation wavelengths. TPA cross-sections were measured using two-photon induced fluorescence measurement technique. The TPA cross-

sections (δ) are determined by comparing their TPEF to that of fluorescein in solvents, according to the following equation [32]:

$$\delta = \delta_{ref} \frac{\Phi_{ref}}{\Phi} \frac{c_{ref}}{c} \frac{n_{ref}}{n} \frac{F}{F_{ref}}$$

Here, the subscripts ref stands for the reference molecule. δ is the TPA cross-section value. *c* is the concentration of solution. *n* is the refractive index of the solution. F is the TPEF integral intensities of the solution emitted at the exciting wavelength, and *F* is the fluorescence quantum yield. The δ_{ref} value of reference was taken from the literature [33].

3 General procedure for the preparation of L1 and L2

L1 and L2 were synthesized by the reactions shown in Fig. 1

4,4'-(1E,1'E)-2,2'-(2-(1H-imidazol-1-yl)pyrimidine-4,6-diyl)bis(ethene-2,1-diyl)bis(N,N-bis(2-(2-methoxyethoxy)ethyl)aniline) L1

0.67 g (6 mmol) t-BuOK was placed into a dry mortar and well milled into powder with heating, then 2-(1H-imidazol-1-yl)-4,6-dimethylpyrimidine **M6** (0.17 g, 1 mmol, seen in SI) and 4-(bis(2-(2-methoxyethoxy)ethyl)amino)benzaldehyde **M4** (1.30 g, 4 mmol, seen in SI) were added and milled vigorously for about 5 min. The sticky crude product was obtained. The mixture was dissolved with CH_2Cl_2 and extracted with water (*ca*. 3×100 mL). Then it was dried with anhydrous $MgSO_4$, filtered, concentrated. The crude product was purified by chromatography on a silica gel with ethyl acetate /ethanol mixture as the eluent. The red sticky product (0.51g) was collected. Yield：65%. IR (KBr, cm^{-1}) selected bands: 3425 (w), 3074 (m), 3037 (s), 2922 (s), 2622 (w), 1602 (s), 1568 (s), 1519 (s), 1468 (s), 1424 (s), 1376 (s), 1322 (s), 1235 (s), 1183 (s), 1109 (s), 1023 (s), 978 (s), 889 (s), 836 (s), 810 (s), 750 (m), 724 (w), 685 (m), 655 (m), 565 (w), 521 (s). ^{1}H-NMR: (400 MHz, CD_3COCD_3), δ (ppm): 3.31 (s, 12H), 3.52 (d, *J* = 4 Hz, 8H), 3.61 (d, *J* = 4 Hz, 8H), 3.69 (s, 16H), 6.85 (d, *J* = 8 Hz, 4H), 7.00 (d, *J* = 16 Hz, 2H), 7.27 (s, 1H), 7.59 (d, *J* = 8 Hz, 4H), 8.06 (d, *J* = 16 Hz, 2H), 7.12 (s, 1H), 8.11 (s, 1H), 8.73 (s, 1H). ^{13}C-NMR (CD_3COCD_3, 100MHz), δ (ppm): 51.76, 58.95, 69.28, 71.24, 72.73, 112.61, 114.14, 117.65, 120.7, 124.2, 130.5, 130.8, 136.89, 139.1, 150.3, 155.3, 166.0. MS: $C_{43}H_{60}N_6O_8$, 788.97, Found: 789.45 ($[M+H]^+$, 46), 811.43 ($[M+Na]^+$, 75) ; MALDI-TOF, m/z (%): 789.29 ($[M+H]^+$,100). Anal. Calcd. For $C_{43}H_{60}N_6O_8$:C,65.46;H,7.67;N,10.65;Found: C,65.41; H, 7.67;N,10.66.

(E)-4-(2-(2-(1H-imidazol-1-yl)pyrimidin-4-yl)vinyl)-N,N-bis(2-(2-methoxyethoxy)ethyl)aniline L2

1.01 g (9 mmol) t-BuOK was placed into a dry mortar and well milled into powder with heating, 2-(1H-imidazol-1-yl)-4-methylpyrimidine **M5** (0.48 g, 3 mmol, seen in SI) and 4-(bis(2-(2-methoxyethoxy)ethyl)amino)benzaldehyde **M4** (1.00 g, 3 mmol, seen in SI) were added to the dry mortar and milled vigorously under the IR LED for about 5 min. The sticky crude product was obtained and was dissolved with CH_2Cl_2, extracted with water (3×100 mL). Then it was dried with anhydrous $MgSO_4$, filtered, concentrated. The crude product was purified by chromatography on a silica gel with petroleum (bp 60-90^{o}C)/ethyl acetate (1:1 by volume) as eluent to yield 0.97 g of red target sticky product. Yield: 69%. ^{1}H-NMR: (400 MHz, CD_3COCD_3), δ (ppm): 3.30 (s, 6H) , 3.48~3.50 (t, *J* =4.6 Hz, 4H), 3.58~3.60 (t, *J* = 4.6 Hz, 4H), 3.67 (s, 8H) , 6.82 (d, *J* = 8.8 Hz, 2H), 7.02 (d, *J* = 15.6 Hz, 1H), 7.11 (s, 1H),7.32 (d, *J* = 5.2 Hz, 1H), 7.58 (d, *J* = 8.4 Hz, 2H), 8.01 (s, 1H), 8.09 (d, *J* = 15.6 Hz, 1H), 8.61 (d, *J* = 5.2 Hz, 1H), 8.63 (s, 1H). ^{13}C-NMR (CD_3COCD_3, 100 MHz, δ/ppm): 51.74, 58.93, 69.25, 71.23, 72.72, 112.6, 116.8, 117.5, 120.0, 123.9, 130.7, 131.1, 136.7, 140.2, 150.5, 155.4, 159.7, 166.2. MS: $C_{25}H_{33}N_5O_4$, 467.56, Found: 468.42 ($[M+H]^+$, 28), 490.42 ($[M+Na]^+$, 83) ; MALDI-TOF, m/z (%): 468.26 ($[M+H]^+$, 100). Anal. Calcd. For $C_{25}H_{33}N_5O_4$:C,64.22;H,7.11;N,14.98;Found:C,65.20; H, 7.11;N,10.99.

Results and discussion

1 Synthesis

Synthetic routes of L1 and L2 and their intermediates are depicted in Fig. 1 and Fig. S1. 4-methylbenzene-1-sulfonyl chloride and 2-methoxyethanol are available commercially. The intermediates M5 and M6 were produced by improved Ullmann reactions in good yield. Compound L1 and L2 were produced by the modified Knoevenagel condensation in the solid phase with t-BuOK as base.

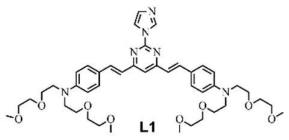
L1

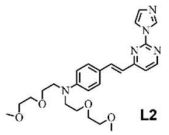
L2

Fig. 1. The molecular structures of L1 and L2.

2 Theoretical calculations

Fig. 2 gives straightforward representations of the electron density distribution. Orbital analysis exhibits that the highest occupied molecular orbital (HOMO) is comprised of π orbitals localized on the benzene and vinyl group. Also the lowest unoccupied molecular orbital (LUMO) distribution is localized in the pyrimidine orbitals with abundant conjugated π-bridge. Hereby, there are relatively strong π-donor interactions between flexible ether oxygen chain and the pyrimidine center, and the electron density in each molecule is very similar. As shown in Fig. 2 and Table S1, the lowest energy absorption band can be assigned to ICT between the nitrogen atom of the amino group and the pyrimidine ring. Basically, the calculated singlet-singlet transitions in all chromophores are in reasonable agreement with the experimental λ_{ab} in the two major absorption bands observed.

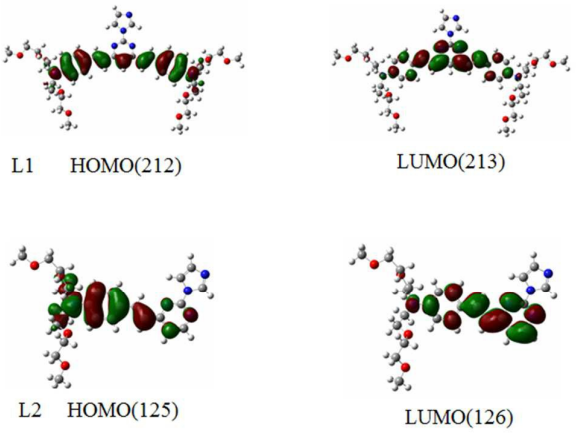

Fig. 2 Representation of calculated HOMO and LUMO orbitals of L1 and L2.

3 Photophysical properties

Fig. 3 and Table 1 lists the UV-Visable and fluorescence spectra of compounds L1 and L2 in several solvents with differing polarities (cyclohexane, benzene, dichloromethane, THF, ethyl acetate, ethanol, acetonitrile, DMF). The concentration of the solution is 1.0×10^{-6}mol L^{-1} .

Solvatochromism

From L1 to L2, the large molar absorption coefficients (log ε_{max}>>4) of the maximum peaks suggested the presence of the π–π* transitions in differing solvents, which is in accordance with theoretical calculations. In addition, these compounds show a pronounced positive solvatochromism [34], resulting in a red-shift of the UV-Vis absorption bands in DMF compared with cyclohexane. Their absorption wavelengths in cyclohexane are located at 429 for L1 and 403 nm for L2, whereas in DMF red-shifted to 444 and 412 nm, respectively. Such solvent-induced shifts are usually interpreted in terms of the different solvation interactions between the polar groups and the solvent, and mainly depend on solvent polarity. The positive solvatochromism is an indicative of a larger stabilization of the excited state as compared to the ground state by a polar solvent, suggesting that a significant charge redistribution takes place upon excitation, which is in accordance with a multidimensional intramolecular charge transfer (MDICT) occurring between the core and the peripheral groups [35]. Moreover, as show in the Fig. 3 and Table 1, the one-photon absorption peak position (λ_{max}) of L1 and L2 show an increasing tendency as polarity of the solvent increase, except in dichloromethane. The OPEF maxima are obtained at their maxima excitation wavelengths in eight different solvents, from which one can see that their emission maxima (λ_{max}^{em}) of L1 and L2 were slightly red shifted with increasing solvent polarity and all the derivatives show definite solvatochromic behavior; for example, for compound L1, the peak wavelength shift from 473nm (cyclohexane) to 557nm (DMF), and for compound L2, from 445 nm (cyclohexane) to 523 nm (DMF) indicating that this charge separation increases in the excited state, resulting in a larger dipole moment than that in the ground state, which can be explained the sensitivity of the emission spectra of these chromophores to solvent polarity accordingly [36] (supported by DFT calculations). Furthermore, the emission of compound (L1) in cyclohexane reveal vibronic definition, and show a progressive red-shift and loss of vibronic structure as the solvent polarity increases[37]. Fig. S2a shows the OPEF intensities of the compound (L1) decrease as polarity of the solvent increase due to solvato-kinetic effect [38]. This can be explained by the fact the larger change in the dipole moment between the excited and the ground state of L1 compared with L2, which means that a strong intramolecular charge transfer existed during the photoinduced process. However, for compound (L2), the OPEF intensities increase with polarity of the solvent increase (Fig. S2b), showing negative solvate-kinetic effect. As is well-known, the negative solvate-kinetic effect is caused by different factors such as

biradicaloid charge transfer [38], the proximity effect [38], and others [39].

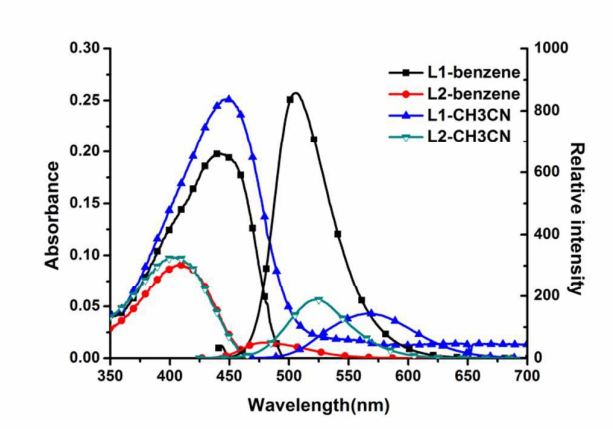

Fig. 3 Single-photon absorption and Single-photon excited fluorescence spectrum of L1 and L2 in benzene and acetonitrile ($c=1\times10^{-6}$mol L^{-1}).

Comparison of branching number

As showed in Fig. S2 and Table 1, from L2 to L1, the one-photon absorption maxima in benzene and in acetonitrile show regular red shifts as the branch number increases. These can be assigned to the more highly extended π-delocalization and a certain coupling between the branches in L1 which can lower the band gaps obviously. Furthermore, the absorption coefficients (ε_{max}) of the maxima increase consistently and significantly and the OPEF spectral intensities are also vary regularly upon increasing the branch number. The intensities of the OPEF of L2 and L1 follow the pattern L1 > L2 in the low polar solvents (benzene) with the ratios of 17.2:1 which is not consistent with branch number [40], while the intensities of the OPEF decrease in the high polar solvents (CH_3CN) from compound (L2) to compound (L1) with the ratios of 1:1.3. These can be explained by negative solvato-kinetic effect of L2. Besides, seen from Table 1, the stokes shifts show monotonically decreasing tendency as the branch number increases, indicating the lone pair electrons on the nitrogen atom of L1 may have delocalized onto the conjugated system and increase intra-molecular charge transfer which could reduce the nonradiative decay channels. These results suggest that compound (L1) is typical D-π-A-π-D chromophores and the nature of peripheral substituting groups (D) have significant influence on their single-photon optical properties.

Lippert-Mataga plot

The magnitudes of dipole moment change (μ_e-μ_g) are proportional to the one photon oscillator strengths, so their values can be calculated from the linear absorption spectrum. However, (μ_e-μ_g) is rarely determined experimentally, so the design of efficient 2PA compounds has proceeded empirically, with guidance from theoretical calculations of transition moments. As seen in Table S2 and Table 1, the fluorescence spectra showed moderate Stokes shifts depending on the solvent polarity. Further, the solvatochromism is observed, suggesting a large change in dipole moment between ground and excited states. The Lippert-Mataga equation is the most widely used to evaluate the dipole moment changes of the dyes with photoexcitation [41].

$$\Delta\nu = \frac{2\Delta f}{4\pi\varepsilon_0\hbar c a^3}(\mu_e - \mu_g)^2 + b$$

$$\Delta f = \frac{\varepsilon - 1}{2\varepsilon + 1} - \frac{n^2 - 1}{2n^2 + 1}$$

in which $\Delta\nu = \nu_{abs} - \nu_{ex}$ stands for the Stokes shifts, ν_{abs} and ν_{ex} are absorption and emission (cm^{-1}), h is Planck's constant, c is the speed of light in a vacuum, a is the Onsager radius and b is a constant. Δf is the orientation polarizability, μ_e and μ_g are the dipole moments of the emissive and ground states, respectively, and ε_0 is the permittivity of the vacuum. $(\mu_e - \mu_g)^2$ is proportional to the slope of the Lippert–Mataga plot. Plots of the Stokes shifts as a function of the solvent polarity factor Δf are shown in Fig. 4. Only the data involving the aprotic solvents are shown because application of this analysis with solvents where specific solute-solvent interactions are present is not appropriate. As shown in Fig. 4, the Lippert–Mataga plot of L1 and L2 give a large slope, which implies larger dipole moment changes with photoexcitation. The slope of the best-fit line is related to the dipole moment change between the ground and excited states (μ_e -μ_g). The slopes of two lines are different: 6086, 7109 cm^{-1} for compounds L1 and L2, respectively. So the values of μ_e μ_g were calculated as 12.3 D for L1, 10.3 D for L2, respectively. The values of the complexes indicate that the molecule in the excited state has an extremely polar structure, an enhanced 2PA response of L1 was found compared with L2, which is in good agreement with their nonlinear optical properties as shown in Table 2.

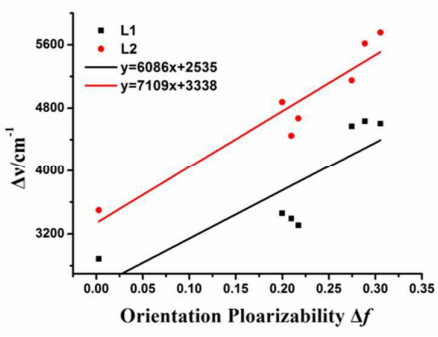

Fig. 4 Lippert–Mataga plots for compounds L1 and L2.

Fluorescence lifetime and quantum yield

To get more insight into the radiative and nonradiative decay processes of L1 and L2, we also conducted time-resolved lifetime experiments (Table 1, Fig. S3).With increasing polarity of the solvents, fluorescence lifetime of the compounds increase generally. These can be explained by the stronger solute/solvent interaction at the excited state comparing with that at the ground state, which indicates that the increasing polarity of the excited state increases. The energy level can be lowered greatly by increasing dipole-dipole interaction between the solute and solvent. The quantum yields (Φ) of the compounds L1 and L2 in different solvents are determined by using Fluorescein as a standard. As shown in Table 1, the quantum yields of compound L1 decrease generally as the polarity of solvent increases except in cyclohexane and benzene, showing the positive solvato-kinetic effect. Note that the quantum yields of L1 obtained in cyclohexane are smaller than that in benzene, because of the negative solvato-kinetic effect. On the contrary, for compound L2, the quantum yield increases generally with solvent polarity, exhibiting negative solvato-kinetic effect.

4 Two-photon excited luminescence (2PEF) spectral properties

It was found that there is no linear absorption in the wavelength range 680~1080nm, indicating that there is no energy level corresponding to an electron transition in the spectral range. Therefore, upon excitation from 680 to 1080 nm, it is impossible to produce single-photon-excited up-converted fluorescence. If frequency upconverted fluorescence occurs upon excitation with a tunable laser in the range 680-1080 nm, it can be safely attributed to multiphoton excited fluorescence. As shown in Fig. S4, a log-log plot of the excited fluorescence signal *versus* excited light power. It provides direct evidence for the squared dependence of excited fluorescence power and input laser intensity upon excitation with a tunable laser in this, therefore, it should be safely assigned to two-photon excited fluorescence (TPEF) for L1 and L2.

By tuning the pump wavelengths incrementally from 720 to 860nm with a step size of 10 nm while keeping the input power fixed and then recording TPEF intensity, TPEF spectra are obtained; the TPEF spectra of L1 and L2 in benzene are shown in Fig.5. It can be seen that the peak position of the TPEF spectra of L1 and L2 are independent of the excitation wavelengths (from 720 to 860nm, Fig S5). The similarities between TPEF and OPEF indicate that both the emissions for a given compound are from the same excited state, though their initial Frank-Condon states may be different. As shown in Fig. 5, the TPEF intensities of these compounds are remarkably stronger than their corresponding OPEF intensities and the TPEF peak wavelengths around 500 and 600 nm of L1 with much higher concentration in benzene are evidently red-shifted by 34-40nm in comparison with those of OPEF in the much lower concentration solution, which can be explained by the reabsorption effect. The short wavelength side of the two-photon fluorescence was reabsorbed by the solution and red-shifts of the fluorescence spectra were readily observed [42]. Moreover, Fig. S6 shows obvious red-shift in the two-photon fluorescence maxima as the polarity of solvent increases of L1 and L2. For L1, The intensities of the TPEF decrease with solvent polarity increase, exhibiting an obvious positive solvate-Kinetic effect. On the contrary, for L2, the intensities of the TPEF increase generally, showing the negative solvate-kinetic effect. Furthermore, It can be seen from Fig. S7 that the intensities of the TPEF increases obviously with the ratios of 1.0:9.3 as the branch number increases, which is a result of extended π-delocalization of L1.

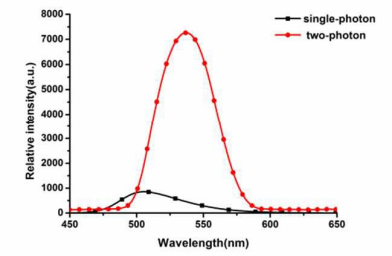

Fig.5 The single-photon and two-photon excited fluorescence spectra of L1 in benzene(c=1×10^{-3}mol L^{-1}).

Table 1 Photophysical properties of chromophores L1 and L2 in several of different polar solvents.

	Solvents	λ_{max} [a]	ε [b]	λ_{max} [c]	Φ [d]	τ [h]	$\Delta\nu$ [i]
L1	cyclohexane	429	7.97	473	0.59	0.51	2196
	benzene	442	1.98	506	0.65	1.04	2887
	dichloromethane	461	2.36	544	0.35	1.67	3310
	THF	449	2.56	529	0.46	2.02	3393
	ethyl acetate	445	2.41	526	0.42	1.64	3461
	ethanol	446	2.25	567	0.11	0.69	4635
	acetonitrile	449	2.52	566	0.10	0.22	4604
	DMF	444	9.77	557	0.17	1.42	4569
L2	cyclohexane	403	9.64	455	0.04	0.09	2867
	benzene	410	9.06	478	0.09	0.24	3500
	dichloromethane	415	9.73	514	0.14	0.65	4670
	THF	413	9.08	506	0.19	0.61	4450
	ethyl acetate	402	9.35	500	0.11	0.44	4876
	ethanol	409	9.20	531	0.24	0.87	5617
	acetonitrile	402	9.86	523	0.25	0.79	5755
	DMF	412	1.12	523	0.23	0.96	5151

[a] Absorption peak position in nm (1×10^{-5} mol L^{-1}). [b] Maximum molar absorbance in 10^{4} mol^{-1} L cm^{-1}. [c] Peak position of SPEF in nm (1.0×10^{-5} mol L^{-1}), excited at the absorption maximum. [d] Quantun yields determined by using coumarin 307 (Φ = 0.56) (1.0×10^{-5} mol L^{-1}) as the standard. [e] fluorescence liftime (ns). [f] Stokes shift in cm^{-1}.

Table 2 Two-photon fluorescence properties of chromophores L1 and L2 in four polar solvents.

	Solvents	λ_{max} [a]	λ_{max} [b]	δ [c]
L1	benzene	532	840	2844

	dichloromethane	558	810	3502
	THF	555	840	3335
	DMF	565	840	2844
L2	benzene	508	840	842
	dichloromethane	524	870	1815
	THF	522	860	1273
	DMF	545	870	842

[a] TPEF peak position in nm pumped by femtosecond laser pulses at 300 mw at their maximum excitation wavelength. [b] 2PA maximum excitation wavelength. [c] 2PA cross section in GM.

The two-photon absorption (TPA) spectra of L1 and L2 complexes are determined in the wavelength range 680-1080 nm in benzene (1.0×10^{-3} mol L^{-1}) by the two-photon-induced fluorescence method with fluorescein as the standard (Fig. 6, Table 2), using two-photon induced fluorescence measurement technique described in the experimental section. The experiments were conducted in the femtosecond regime, thereby preventing contribution from linear nonresonant absorption or from excitedstate absorption. As shown in Fig. 6 and Table 2, the two-photon absorption cross sections (δ) are dependent over excitation wavelengths (from 720 to 860nm). The details of determination conditions and theoretical calculations are given in the Experimental Section. The largest δ is 2844 GM (1GM = 10^{-50} cm^4 s $photon^{-1}$) in benzene solution for L1, which is similar to Goodson's value [21]. The maximum two-photon absorption cross-section is 842 GM for L2 in benzene solution which is in line with the results of theoretical calculation about $\Delta\mu$, as mentioned above. Compared with L2, L1 bearing the much larger 2PA cross-section may imply that extending π-conjugation domain accomplished by increasing the number of branches of a chromophore molecule based on the structural motif of a multi-branched olefin could be a useful approach toward enhanced molecular nonlinear absorptivities. With respect to our system, L1 accomplished a large 2PA cross-section (2844 GM) which attributed to the fact that the branched chromophore has an extended π-conjugated system compared to that of L2 [43]. Compared with our previous work[30], the 2PA cross-section of L1 with Eher oxygen chains is higher than the ehyl substituent pyrimidine derivative Z2 (1879 in benzene), such a difference must be due to varied substituent group of the pyrimidine-based chromophores, which may arise from the strong electron-donating effect of L1.

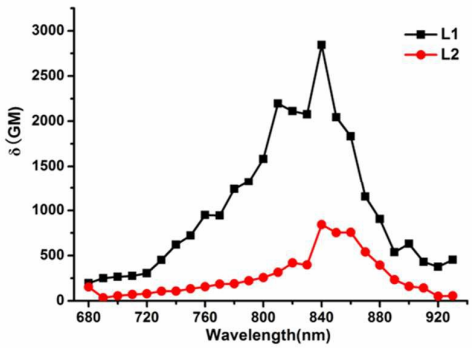

Fig.6 TPA cross section of L1 and L2 in benzene (c=1×10-3mol L-1) versus excitation wavelengths.

The TPA cross-section values (δ) increases obviously as the branch number increases with the ratios of 1.0:3.5 from L2 and L1 (Fig. 6). The 2PA cross-section δ/MW is divided by the molecular weight, varies in a proportion of 1.0:2.0. This means that the unit molecular weight enables enhanced TPA cross-section values as the branch number increases, which leads to the indication of some interactions between branches in the molecule. The solvent-dependent of the two-photon absorption cross section value was reported by Bazan *et al*. [44] and our group [45]. Fig. S8 and Table

2 reveals that the two chromophores exhibit a discernible TPA spectral feature in different solvents. L2 in high polar solvent (DMF) shows its maxima TPA cross-section of 1192 GM. Increasing the polarity of solvents leads to a remarkable increase of TPA cross-section due to negative solvate-Kinetic. For compound (L1), the maxima TPA cross-section values (3357 GM) were observed in the solvent with moderate polarity (THF) [46]. These data indicate that electronic excitation augments pyrimidine-based chromophores electron density via an internal charge transfer mechanism due to solvent effects. Consequently, compound L1 has the cooperative effects in both linear and non-linear TPA process, which has been verified by Beljonne's exciton model [47]. The extra enhancement in TPA response for L1 can be achieved when the core allows significant electronic coupling rather than L2.

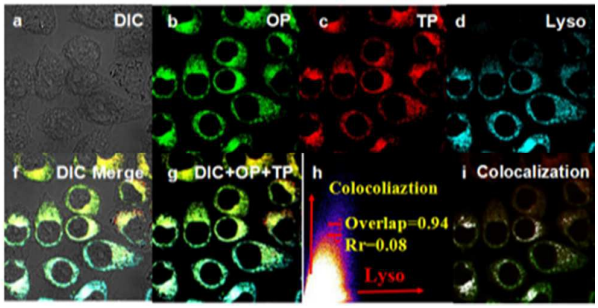

Fig. 7 (a**)** Bright-field image of HepG2 cells. (b) One-photon image of HepG2 cells incubated with 20 μL1 after 60 min of incubation, washed by PBS buffer. λex = 458 nm (emission wavelength from 525 to 625 nm). (c) Two-photon image of HepG2 cells incubated with 20 μL after 60 min of incubation, washed by PBS buffer. λex = 840 nm (emission wavelength from 500 to 600 nm). (d) One-photon image of HepG2 cells incubated with Lysotracker®. λex = 633 nm (emission wavelength from 660 to 700 nm). (f) The overlay of (a) to (d). (g) The overlay of (a) to (c). (h,i) Co-localization micrograph profile prove that the co-staining region which is located in cell cytosol.

5. Cell image and cytotoxicity assay

To search for the potential application of L1 and L2 in bioimaging, cytotoxicities of the chromophores were measured toward the human cervical carcinoma cells HepG2. Because of low aqueous solubility, the tested compounds were dissolved in DMSO first and then serially diluted in complete culture medium such that the effective DMSO content did not exceed 1%. These data show that HepG2 cells show near 100% viability following 24 h of treatment with 10 μM L1. Higher concentrations result in decreased cell survival, with 65% and 53% viability observed following 24 h of treatment with 40 μM L1 and L2 (Fig. S9). These cytotoxicity tests show that sub- and low-micromolar concentrations of L1 are related low toxic over a period of at least 24 h and could be safely used for further biological studies (Fig. 7). A co-staining experiment with Lysotracker® was performed to further determine that whether L1 was internalized with lysochondria (Fig. 7 (d)). At the same time, TPM images were obtained from HepG2 cells incubated with L1, owing to its relatively low toxicity toward live cells, high quantum yield, large TPA cross-section and long fluorescent lifetime. Fluorescent images of confocal microscopy and TPM of HepG2 cells labeled with L1 were captured. A bright-field image (Fig. 7(a)) of each cell was taken immediately prior to the one-photon and TPM imaging. The green red channel clearly reveals HepG2 cells successfully uptake L1, and interestingly, the luminescence located in cell cytosol (Fig. 7(b) and (c)). The unusual two-photon luminescent properties and the low cytotoxicity of L1 make it a potential candidate as novel luminescence material for live cell imaging.

Conclusion

In brief, two pyrimidine derivatives with D–π-A–π-D and D–π-A configuration have been synthesized by convenient method. The chromophores showed good one and two-photon excited fluorescence behaviour and interesting solvatochromic properties. The centrosymmetric charge transfer D–π-A–π-D structural chromophore L1 exhibited relatively large TPA cross-section, strong two-photon-induced fluorescence. The TPA cross-section of the molecules tend to tone up with the increasing of conjugation length and the donor strength. The compound L1 with a lower molecular weight exhibits higher quantum yield, larger 2PA cross section in the near-infrared region, higher photo-stability, lower toxicity and brighter two-photon fluorescent bioimaging, was successfully applied to a two-photon fluorescent probe for labeling the cytoplasm in live cells. We believe that the design method and fabrication strategy are potentially applicable to the derivatization of analogous two-photon absorption chromophores.

Acknowledgement

This work was supported by grants from the National Natural Science Foundation of China (21501001, 21271004, 51372003, 51432001, 21271003, 51072001, 81503009 and 51272001), National Key Basic Research Program 973 (2013CB632705), Ministry of Education Funded Projects Focus on returned overseas scholar, Program for New Century Excellent Talents in University (China) and Doctoral Program Foundation of Ministry of Education of China (20113401110004), China Postdoctoral Science Foundation (2015M571912), the Swedish Research Council (VR) (621-2013-5357) and Swedish Government strategic faculty grant in material science (SFO, MATLIU) in Advanced Functional Materials (AFM), the Wenner-Gren Foundations.

References

[1] P. Chantharasupawong, R. Philip, N. T. Narayanan, P. M. Sudeep, A. Mathkar, P. M. Ajayan, *et al*. *J. Phys. Chem. C.,* **2012**, 116, 25,955-25,961.

[2] F. Q. Guo, W. F. Sun, *Inorg. Chem.,* **2005**, 44, 4055-4065.

[3] (a)J. Arnbjerg,M. Johnsen, P. K.Frederiksen, S. E Braslavsk and P. R.Ogilby, *J. Phys. Chem. A.* **2006**, 110, 7375-7385. (b) L.Beverina, M. Crippa, M. Landenna, R. Ruffo, P. Salice, F. Silvestri, S. Versari, A.Villa, L.Ciaffoni, E. Collni,C. Ferrante, S.Bradamante, C. M. Mari, T. Bozio and G. A.Pagani, *J. Am. Chem. Soc.*, **2008**, 130, 1894-1902.

[4] (a) S. Kim, T. Y. Ohulchanskyy, H. E. Pudavar, R. K. Pandey, P. N. Prasad, *J. Am. Chem. Soc.,* **2007**, 129, 2669-2675.(b) L. Li, C. W. Zhang, G. Y. J. Chen, B. W. Zhu, C. Chai, Q. H. Xu, E. K. Tan, Q. Zhu, K. L. Lim, and Q. Y. Shao, *Nat. Commun.*, **2014**, 5, 3276-3285

[5] (a) L. Donato, A. Mourot, C. M. Davenport, C. Herbivo, D. Warther, J. Léonard, F. Bolze, J. -F. Nicoud, R. H. Kramer, M. Goeldner and A. Specht, Angew. Chem., **2012**, 51(8), 1840-1843. (b) G. Bort, T. Gallavardin, D. Ogden and P. I. Dalko, *Angew. Chem.,* **2013**, 52(17), 4526-4537.

[6] (a) Kim, H. M. and Cho, B. R, Chem. Rev. **2015**, 115, 5014−5055.(b) X. Yue, Z. Armijo, K. King, M. V. Bondar, A. R. Morales, A. Frazer, I. A. Mikhailov, O. V. Przhonasa and K. D. Belfield, ACS Appl. Mater. Interfaces., **2015**, 7, 2833-2846.

[7] K. A. S. Dvornikov, E. P. Walker and P. M. Rentzepis, *J. Phys. Chem. A.*, **2009**, 113, 13633-13644.

[8] Z. Q. Li, N. Pucher, K.Cicha, J.Torgensen. S. C. Ligon, A. Ajami, W. Husinsky, A. Rosspeintner, E. Vauthey, S. Naumov, T.Scherzer, J. Stampfl, and R. Liska, *Macromolecules*., **2013**, 46, 352-361.

[9] J. Lott, C. Ryan, B. Valle, J. R. Johnson III, D. A. Schiraldi, J. Shan, *et al., Adv. Mater.,* **2011**, 23, 2425-2429.

[10] M. Stoneman, M. Fox, C. Y. Zeng, V. Raicu, *Lab. Chip.,* **2009**, 9, 819-827.

[11] J. E. Koskela, S. Turunen, L. Ylä Outinen, S. Narkilahti, M. Kellomäki, *Polym. Advan. Technol.,* **2012**, 23, 992-1001.

[12] (a) H. Zhang, J. Fan, J. Wang, S. Zhang, B. Dou and X. Peng, *J. Am. Chem. Soc.,* **2013**, 135, 11663–11669**;** (b) W. Zhang, P. Li, F. Yang, X. Hu, C. Sun, W. Zhang, D. Chen and B. Tang, *J. Am. Chem. Soc.*, **2013**, 135, 14956–14959.

[13] H.-Y. Ahn, K. E. Fairfull-Smith, B. J. Morrow, V. Lussini, B. Kim, M. V. Bondar, S. E. Bottle and K. D. Belfield, *J. Am. Chem. Soc.*, **2012**, 134, 4721–4730**;**

[14] L. Li, J. Ge, H. Wu, Q. H. Xu and S. Q. Yao, *J. Am. Chem. Soc.*, **2012**, 134, 12157–12167;

[15] D. E. Kang, C. S. Lim, J. Y. Kim, E. S. Kim, H. J. Chun and B. R. Cho, *Anal. Chem.,* **2014**, 86, 5353-5359.

[16] M. Collot, C. Loukou, A. V. Yakovlev, C. D. Wilms, D. Li,A. Evrard, A. Zamaleeva, L. Bourdieu, J.-F. L´eger, N. Ropert,J. Eilers, M. Oheim, A. Feltz and J.-M. Mallet, *J. Am. Chem.Soc.*, **2012**, 134, 14923–14931.

[17] L. Y. Zhou, X. B. Zhang, Q. Q. Wang, Y. F. Lv, G. J. Mao, A. L. Luo, Y. X. Wu, Y. Wu, J. Zhang and W. H. Tan, *J. Am. Chem. Soc.*, **2014**, 136, 9838–9841.

[18] B. A. Reinhardt, L. L. Brott, S. J. Clarson, A. G. Dillard, J. C. Bhatt, R. Kannan, *et al*., *Chem. Mater.,* **1998**, 10, 1863-1874.

[19] A. Abbotto, L. Beverina, R. Bozio, A. Facchetti, C. Ferrante, G. A. Pagani, D. Pedron, R. Signorini, *et al*., *Org. Lett.,* **2002**, 4, 1495-1498.

[20] M. Drobizhev, A. Karotki, A. Rebane, C. W. Spangler, *Opt. Lett.,* **2001**, 26, 1081-1083.

[21] I. Polyzos, G. Tsigaridas, M. Fakis, V. Giannetas, P. Persephonis, J. Mikroyannidis, *Chem. Phys. Lett.,* **2003**, 369, 264-268.

[22] D. W. Brousmiche, J. M. Serin, J. M. J. Frechet, G. S. He, T. C. Lin, S. J. Chung, *et al*., *J. Am. Chem. Soc.,* **2003**, 125, 1448-1449.

[23] S. J. Chung, K. S. Kim, T. C. Lin, G. S. He, J. Swiatkiewicz, P. N. Prasad, *et al*., *Chem. Mater.,* **2001**, 13, 4071-4076.

[24] A. Bhaskar, G. Ramakrishna, Z. K. Lu, R. Twieg, J. M. Hales, D. J. Hagan, *et al*., *J. Am. Chem. Soc.,* **2006**, 128, 11840–11849.

[25] B. R. Cho, K. H. Son, S. H. Lee, Y. S. Song, Y. K. Lee, S. J. Jeon, *et al*., *J. Am. Chem. Soc.,* **2001**, 123, 10039-10045.

[26] (a) B. Liu, H. L. Zhang, J. Liu, Y. D. Zhao, Q. M. Luo, Z. L. Huang, *J. Mater. Chem.,* **2007**, 17, 2921-2929. (b) H. Akdas-Kilig, T. Roisnel, I. Ledoux, H. L. Bozec, *New. J. Chem.,* **2009**, 33, 1470-1473

[27] (a) Z. J. Liu, T. Chen, B. Liu, Z. L. Huang, T. Huang, S. Y. Li, *et al*. *J. Mater. Chem.,* **2007**, 17, 4685-4689.(b) S.Achelle and C. Baudequin, Targets in Heterocyclic Systems-Chemistry and Properties, 2013,17,1-215. (c) S. Achelle and N. Ple, Current Organic Synthesis., **2012**, 9, 163-187.

[28] (a) Z. J. Liu, P. Shao, Z. L. Huang, B. Liu, T. Chen, J. G. Qin. Chem. Commun., **2008**, 2260-2262.(b) L. Li, Y. P. Tian, J. X. Yang, P. P. Sun, L. Kong, J. Y. Wu, Chem. Commun., **2010**, 46, 1673-1675.(c)J. -P. Malval, S. Achelle, L. Bodiou, A. Spangenberg, L. C. Gomez, O. Soppera and F. R. Guen, J. Mater. Chem. C., **2014**, 2, 7869-7880.

[29] (a) X. Y. Zhou, S. Khanapur, A. P. Huizing, R. Zijlma, M. Schepers, R. A. J. O. Dierckx, A. Van Waarde, E. F. J. De. Vries and P. H. Elsinga, J. Med. Chem., **2014**, 57, 9204-9210. (b) L. Y. Ma, Y.-C. Zheng, S. -Q. Wang, B. Wang, Z.-R. Wang, L.-P. Pang, M. Zhang, J. -W. Wang, L. Ding, J. Li, C. Wang, B. Hu, Y. Liu, X.-D. Zhang, J. -J. Wang, Z. -J. Wang, W. Zhao and H. -M. Liu, J. Med. Chem., **2015**, 58, 1705-1716.

[30] C. Tang, Q. Zhang, D. D. Li, J. Zhang, P.F. Shi, S. L. Li, J. Y. Wu and Y. P. Tian, Dyes and Pigments., **2013**, 99, 20-28.

[31] J. N. Demas, G. A. Crosby, *J. Phys. Chem.,* **1971**, 75, 991-1024.

[32] C. Xu, W. W. Webb, *J. Opt. Soc. Am. B.,* **1996**, 13, 481-491.

[33] O. Varnavski, T. Goodson III, L. Sukhomlinova, R. Twieg, *J. Phys. Chem. B.,* **2004**, 108, 10,484-10,492.

[34] C. Hadad, S. Achelle, J. C. García-Martinez, J. Rodríguez-López., *J. Org. Chem.,* **2011**, 76, 3837–3845.

[35] J. Brunel, O. Mongin, A. Jutand, I. Ledoux, J. Zyss, M. Blanchard-Desce, *Chem. Mater.,* **2003**, 15, 4139-4148.

[36] (a) B. Liu, Q. Zhang, H. J. Ding, G. J. Hu, Y. J. Du, C. K. Wang, *et al*., *Dyes. Pigm.,* **2012**, 95, 149-160. (b) B. Wang, Y. C. Wang, J. L. Hua, Y. H. Jiang, J. H. Huang, S. X. Qian, *et al*., *Chem. Eur. J.,* **2011**, 17, 2647-2655.

[37] (a) A. Demeter, S. I. Druzhinin, S. A. Kovalenko, T. A. Senyushkina, K. A. Zachariasse, *J. Phys. Chem. A.,* **2011**, 115, 1521–1537. (b) K. A. Zachariasse, S. I. Druzhinin, W. Bosch, R. Machinek., *J. Am. Chem. Soc.,* **2004**, 126, 1705-1715.

[38] C. G. Niu, A. L. Guan, G. M. Zeng, Y. G. Liu, Z. W. Li, *Anal. Chim. Acta.*, **2006**, 577, 264-270.

[39] Z. Li, S. K. Wu, *J. Fluoresc.*, **1997**, 7, 237-242.

[40] E. Collini, *Phys. Chem. Chem. Phys.,* **2012**, 14, 3725-3736.

[41] S. A. Patel, M. Cozzuol, J. M. Hales, C. I. Richards, M. Sartin, J. C. Hsiang, *et al*., *J. Phys. Chem. C.,* **2009**, 113, 20264-20270.

[42] F. Xu, Z. W. Wang, Q. H. Gong, *Opt. Mater.,* **2007**, 29, 723-727.

[43] (a) P. Milosz, A. C. Hazel, G. D. Robert, L. A. Harry, Angew. Chem. Int. Ed., **2009**, 48, 3244-3266. (b) S. J. Chung, K. S. Kim, T. C. Lin, G. S. He, J. Swiatkiewicz, P. N. Prasad, J. Phys. Chem. B., **1999**, 103, 10741-10745. (c) K. D. Belfield, M. V. Bondar, A. R. Morales, A. Frazer, I. A. Mikhailov, O.V. Przhonska, J. Phys. Chem. C., **2013**, 117, 11941-11952. (d) Y. P. Xie, X. F. Zhang, Y. D. Zhang, F. Zhou, J. Qi, J. L. Qu, Chem. Commun., **2012**, 48, 4338-4340. (e) S. Achelle, J.-P. Malval, S. Aloise, A. Barsella, A. Spangenberg, L. Mager, H. Akdas-Kilig, J.-L. Fillaut, B. Caro and F. R. Guen, ChemPhysChem., **2013**, 14, 2725-2736. (f)L. Li, Y. P. Tian, J. X. Yang, P. P. Sun, J. Y. Wu, H. P. Zhou, S. Y. Zhang, B. K. Jin, X. J. Xing, C. K. Wang, M. Li, G. H. Cheng, H. H. Tang, W. H. Huang, X. T. Tao and M. H. Jiang, Chem. Asian. J., **2009**, 4, 668-680.

[44] H. Y .Woo, B. Liu, B. Kohler, D. Korystov, A. Mikhailovsky, G. C. Bazan, *J. Am. Chem. Soc.,* **2005**, 127, 14,721-14,729.

[45] X. C. Wang, X. H. Tian, Q. Zhang, Y. P. Tian, P. P. Sun, J. Y. Wu, *Chem. Mater.,* **2012**, 24, 954-961.

[46] J. J. Shao, Z. P. Guan, Y. L. Yan, C. J. Jiao, Q. H. Xu, C. Y. Chi, *J. Org. Chem*. **2011**, 76, 780-790.

[47] D. Beljonne, W. Wenseleers, E. Zojer, Z. G. Shuai, H. Vogel, S. J. K. Pond, *et al*. *Adv. Funct. Mater.,* **2002**, 12, 631-641.

Design, synthesis, linear and nonlinear photophysical properties of novel pyrimidine-based imidazole derivatives

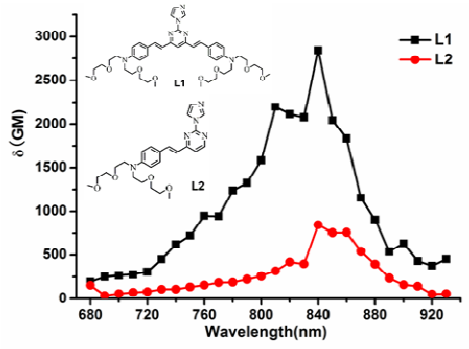

L1 exhibited relatively large TPA cross-section rather than L2, which can be applied for labeling the cytoplasm in live cells.